IEEE International Workshop on Intelligent Robots and Systems
IROS '90

Dynamic Walk Control of a Biped Robot along the Potential Energy Conserving Orbit

Shuuji Kajita, Kazuo Tani and Akira Kobayashi†

Mechanical Engineering Laboratory
Namiki 1-2, Tsukuba, Ibaraki 305, Japan
† Department of Control, Tokyo Institute of Technology
Ohokayama 2-12-1, Meguro-ku, Tokyo 152, Japan

ABSTRACT: To reduce the complex walking dynamics of a biped, we note a particular class of trajectories that is derived by application of gravity compensation to an ideal biped model. The trajectories have following properties: (a) the center of gravity of the body moves horizontally, and (b) the horizontal motion of the center of gravity can be expressed by a simple linear differential equation.

The trajectory on which the center of gravity moves is named the potential energy conserving orbit. Based on its simple dynamics, the control laws for the dynamic biped walk are formulated. It is shown that the walking motion is determined by the support leg exchange. Moreover, robust realization of the walking control is considered.

An experimental walking machine was designed as a nearly ideal biped model. To make the legs light, the legs were the parallel link structures so that their DC motors were mounted in the body. As the results of the experiment, dynamic walking including walk initiation and four steps was achieved.

1. INTRODUCTION

A biped walking robot has high-order and nonlinear dynamics. Therefore, it is difficult to design its dynamic gait and control system. There have been many theoretical and experimental studies [1]-[9] on deriving stable gait control.

An effective approach is to divide the system model into simpler subsystems. Golliday and Hemami decoupled the original high-order system dynamics into independent low-order subsystems using state feedback [4]. Miyazaki and Arimoto used a singular perturbation technique, and showed that biped locomotion can be divided into two modes: a fast mode and a slow mode [5]. Furusho and Masubuchi derived a reduced order model as a dominant subsystem which approximates the original high-order model very well by application of local feedback at each articular joint of the biped robot [6].

Another technique to reduce the complexity of the biped dynamics was shown by Gubina, Hemami, and McGhee [3]. They described an example in which specific computed torque can reduce the dynamics of an ideal biped without any approximation.

In this paper, we propose the potential energy conserving orbit with global linear dynamics as a special class of the trajectories of an ideal biped model. It is derived by application of specific computed torques to the ideal model like the method of Gubina et al., but we obtain far more simple dynamics. It is easy to get strict analytical solution of the potential energy conserving orbit, and it is effective on designing biped walking motions.

As our theory premises an ideal robot with massless legs, we developed an experimental biped robot whose legs are designed as light as possible. Finally, we show the results of our experiments with this biped robot.

2. GLOBAL LINEARIZATION OF THE IDEAL BIPED MODEL

Figure 1 shows an ideal biped model consisting of a single rigid body with mass m and moment of inertia J, and two massless legs of variable length. The variable length leg simply represents the function of the knee or the effect of kick action. We assume the motion of the model is constrained to a sagittal plane which is defined by the vertical axis and the axis of walking direction. Moreover, we consider the case that the robot is in the single leg support phase.

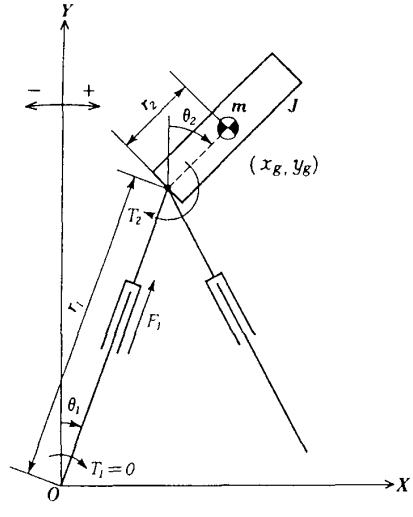

Fig. 1 Ideal biped model

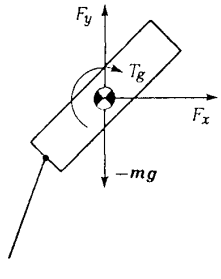

Fig. 2 Forces acting on the body

Since we do not assume any actuator at the foot, the torque around the ankle joint is zero (T_1=0). F_1 is an input force applied along the leg, and T_2 is the hip torque acting between the leg and the body. The force components and torque which drive the body caused by F_1 and T_2 are denoted as F_x, F_y, and T_g in the coordinates shown in Fig. 2, and are expressed as follows.

$$F_x = F_1\sin\theta_1 - (\frac{T_1}{r_1})\cos\theta_1 \tag{1}$$

$$F_y = F_1\cos\theta_1 - (\frac{T_2}{r_1})\sin\theta_1 \tag{2}$$

$$T_g = -F_1 r_2\sin(\theta_1 - \theta_2) + T_2((\frac{r_2}{r_1})\cos(\theta_1 - \theta_2)+1) \tag{3}$$

To compensate for the gravitational force acting on the center of gravity of the body and to keep posture of the body, we assume following conditions.

$$F_y = mg \tag{4}$$

$$T_g = 0 \tag{5}$$

Substituting these conditions into eqs. (2) and (3) and solving for F_1 and T_2, we obtain

$$F_1 = \frac{mg(r_1 + r_2\cos(\theta_1 - \theta_2))}{r_1\cos\theta_1 + r_2\cos\theta_2} \tag{6}$$

$$T_2 = \frac{mgr_1r_2\sin(\theta_1 - \theta_2)}{r_1\cos\theta_1 + r_2\cos\theta_2} \tag{7}$$

By applying F_1 and T_2, the body moves horizontally and keeps a constant posture during its motion if the y component of the initial velocity and the initial angular velocity of the body are both equal to zero (Fig. 3).

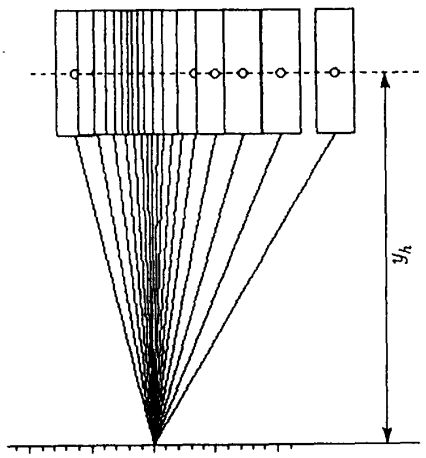

Fig. 3 Linearized motion

Since we assume the ankle torque T_1 is zero at this gravity compensation, the effect of the gravitational force appears as F_x, the force acting horizontally to the center of gravity (C.G.) of the body. Substituting eqs. (6) and (7) into eq. (1), we obtain

$$F_x = \frac{mg(r_1\sin\theta_1 + r_2\sin\theta_2)}{r_1\cos\theta_1 + r_2\cos\theta_2} \tag{8}$$

It is obviously

$$r_1\sin\theta_1 + r_2\sin\theta_2 = x_g$$

$$r_1\cos\theta_1 + r_2\cos\theta_2 = y_g$$

$$F_x = m\ddot{x}_g$$

where (x_g, y_g) is the location of the C.G. of the body. Substituting these equations into eq. (8), we obtain the motion equation of the C.G. of the body.

$$\ddot{x}_g = g\frac{x_g}{y_g} \tag{9}$$

As we have already shown, under the particular initial condition the body moves horizontally. In such case, we obtain a linear differential equation of x_g.

$$\ddot{x}_g = (\frac{g}{y_h})x_g \tag{10}$$

where y_h is constant vertical distance between the C.G. of the body and the ground.

Notice that eqs. (9) and (10) only depend on the position of the C.G. of the body and gravitational acceleration g. They do not depend on the physical parameters of the body: mass m and moment of inertia J.

3. POTENTIAL ENERGY CONSERVING ORBIT

We name the class of the trajectories described by eq. (10) a *potential energy conserving orbit* because the body moves along a horizontal line. We will investigate this orbit for designing the dynamic walking of the biped robot.

If the initial position $x_g(0)$ and the initial velocity $\dot{x}_g(0)$ are given, the motion of the C.G. of the body is presented by an analytical solution of eq. (10) as follows.

$$x_g(t) = x_g(0)\cosh(t/T_c) + T_c\dot{x}_g(0)\sinh(t/T_c) \tag{11}$$

$$\dot{x}_g(t) = (x_g(0)/T_c)\sinh(t/T_c) + \dot{x}_g(0)\cosh(t/T_c) \tag{12}$$

where $T_c = \sqrt{y_h/g}$.

Equations (11) and (12) can be used for predicting the motion of the robot. Another useful equation for designing biped walk is derived by multiplying eq. (10) by $\dot{x}_g$ and integrating it.

$$\frac{1}{2}\dot{x}_g^2 - \frac{g}{2y_h}x_g^2 = constant \equiv E \tag{13}$$

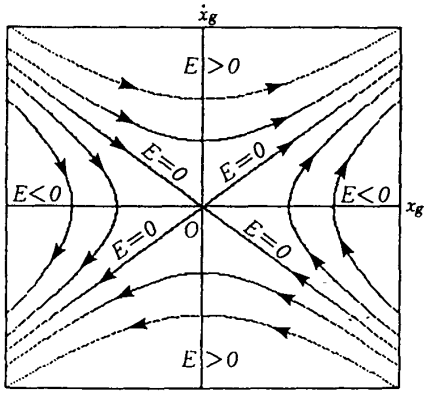

Fig. 4 Phase plane trajectories

Equation (13) shows that a kind of energy is conserved, and we call this the *orbital energy*. Clearly, the first term of eq. (13) represents the kinetic energy per unit mass of the body. The second term is regarded as the virtual potential energy caused by the force field that generates a force $(g/y_h)x$ on the unit mass located at x.

The trajectories of the potential energy conserving orbits are characterized by the value of the orbital energy (Fig. 4). When $E>0$, the body swings from the minus side to the plus side of the x-axis or the other way. $E=0$ represents the equilibrium state ($x_g=0$, $\dot{x}_g=0$), the state swing toward the equilibrium point, or the swing out of the equilibrium point. When $E<0$, the body never passes the point $x=0$. In such case, the trajectories have a turning point at which the velocity of the body becomes zero.

4. DESIGN OF THE DYNAMIC WALKING LOCOMOTION

For the gait of the biped model in Fig. 1, we assume a *singular gait* in which, during walking, the body is supported by only one of the legs at any time [3]. In addition, we assume that the velocity of the body just after the support leg exchange is equal to the velocity just before exchange.

Parameters at the instant of n-th exchange of the support leg are defined as shown in Fig. 5, where s_{n+1} denotes the length of the new step, v_{ex} the velocity at the exchange, and x_{fn} the location of the C.G. of the body.

The value of the orbital energy E can be changed only at the support leg exchange. The relationship between the exchanging conditions and the value of E is derived as follows. Denoting the orbital energy before and after the exchange E_n and E_{n+1}, they are represented as

$$E_n = \frac{1}{2}v_{ex}^2 - \frac{g}{2y_h}x_{fn}^2 \tag{14}$$

$$E_{n+1} = \frac{1}{2}v_{ex}^2 - \frac{g}{2y_h}(x_{fn}-s_{n+1})^2 \tag{15}$$

By eliminating v_{ex} from eqs. (14) and (15), we obtain

$$x_{fn} = \frac{y_h}{gs_{n+1}}(E_{n+1}-E_n)+\frac{s_{n+1}}{2} \tag{16}$$

If a particular walking sequence is given by $(E_0, E_1, \ldots, E_n)$ and $(s_1, s_2, \ldots, s_n)$, we obtain leg support exchanging conditions $(x_{f0}, x_{f1}, \ldots, x_{fn-1})$ that realize the specified walking, using eq. (16).

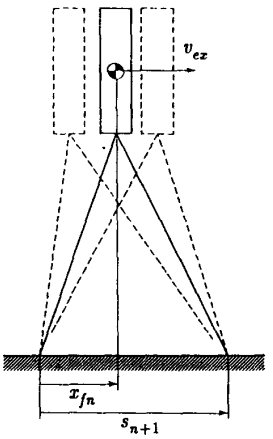

Fig. 5 N-th support leg exchange

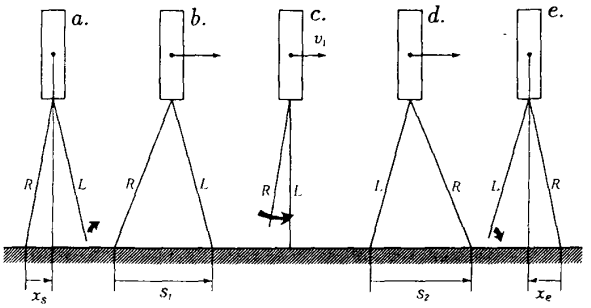

Fig. 6 Specification of the walking

For example, let us consider an ideal walking robot that takes one step forward and then stops (Fig. 6). In this case, the support leg exchange occurs twice, and three orbital energies have to be defined. During the walk initiation phase (a-b), the orbital energy is calculated from the initial position of the body.

$$E_0 = -\frac{g}{2y_h}x_s^2$$

From the first support leg exchange until the next (b-c-d), we specify the typical walking speed v_1 which is the velocity at the moment when $x_g = 0$ (c).

$$E_1 = \frac{1}{2}v_1^2$$

During the walk termination phase (d-e), the orbital energy is calculated from the final position at which the speed of the body becomes zero.

$$E_2 = -\frac{g}{2y_h}x_e^2$$

With these specifications, the first leg exchanging condition x_{f0} is calculated by substituting E_0, E_1, and s_1, the first step length, into eq. (16). Next, x_{f1} is calculated from E_1, E_2, and s_2, the second step length. The entire walking sequence thus calculated is shown in Fig. 7. In this figure the body displacement along the x-axis is evaluated as the distance from each contact point of the support leg.

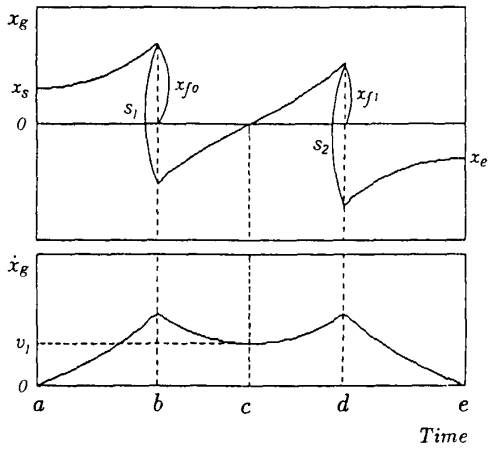

Fig. 7 Designed motion

5. SIMULATION

We carried out a simulation to design the control system. Figure 8 shows the simulated model, which is a simplified model of the experimental robot described in the next chapter. Each leg of the model is a parallel link structure made of four fixed length links, and driving torques T_2 and T_3 are independent coaxial torques applied from the body as the arrows show in the figure. Except the configuration of the legs, we use the same assumption that is used in Chapters 2-4. Those are (i) massless legs, (ii) singular gait, and (iii) no change of the velocity of the body at the support leg exchange.

For the control law of the simulated model, we use local PD feedback for each joint.

$$T_i = f_p(q_i^*-q_i)+f_d(-q_i) \quad (i=2,3) \tag{17}$$

where f_p and f_d are proportional and derivative feedback gains selected to make the response fast enough with respect to the walking motion and with small overshoot. q_i^* is a reference angle for q_i. To generate the potential energy conserving orbit, we give the reference angles as follows.

$$q_2^* = -q_1 \tag{18}$$

$$q_3^* = \sin^{-1}((y_H-r_3-r_1\cos q_1)/r_2)-\pi/2 \tag{19}$$

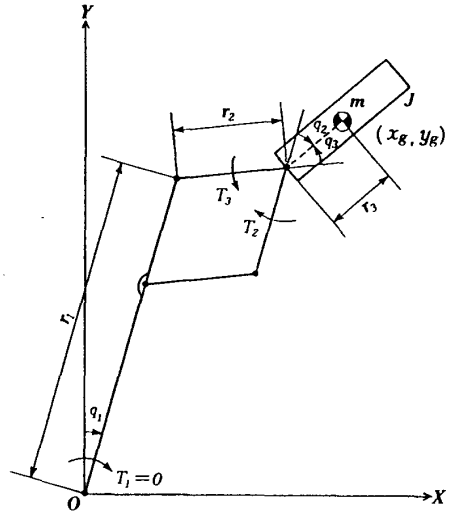

Fig. 8 Simulated model

r_1 (cm)	30.0
r_2 (cm)	10.0
r_3 (cm)	4.0
m (g)	2.0×10^3
J (g.cm^2)	1.0×10^5

Table 1 Parameters for simulation

where y_H is the specified height of the C.G. of the body from the ground surface. q_2^* and q_3^* are calculated from q_1, the angle of the ankle joint. Under this control law, the body moves horizontally and keeps the vertical posture, and we assume that the horizontal motion of the body is represented by eq. (10).

The results of the simulation of four walking steps are shown in Fig. 9(a). Broken lines show the ideal trajectory calculated from eq. (10). It is ascertained that the potential energy conserving orbit is approximately realized under the control law (17)-(19). Figure 9(b) shows the vertical reaction force from the floor in the same simulation. It is almost equal to the robot weight which is shown by a broken line except just after the support leg exchange. Since the vertical reaction force from the floor is always positive in Fig. 9(b), it is ascertained that walking motion of the robot can be realized with its leg kept in contact with the floor (assuming that enough frictional force prevents slipping between the foot and the ground).

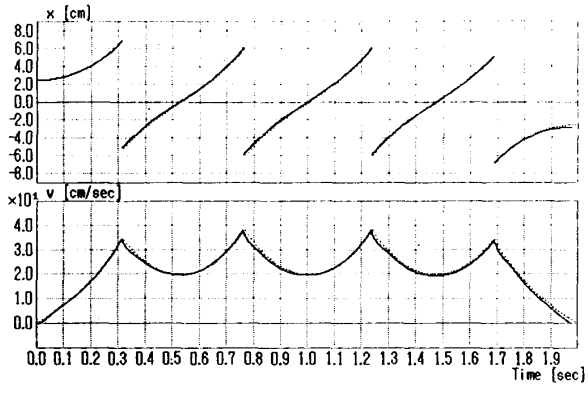

(a) Horizontal motion of the center of gravity (y_H=34.1)

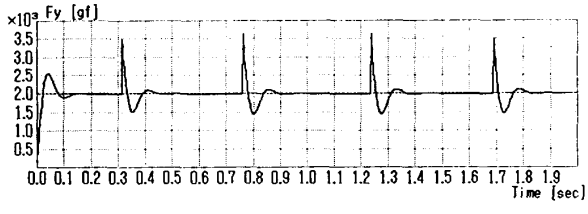

(b) Vertical reaction force from the floor

Fig. 9 Simulated dynamic walking

6. EXPERIMENTAL SYSTEM

6.1 Hardware

The experimental walking robot was designed to move in the sagittal plane. The robot has the legs of the parallel link structure which are driven by four DC servo motors mounted on the body (Figs. 10 and 11). The ankle joint of each leg has no actuator, but potentiometer. It measures angles between the robot and the ground during the support phase of each leg. Four potentiometers are mounted on the joint of the parallel link for the servo control.

The aim in employing the parallel link structure is to approximate the massless leg model as closely as possible by reducing the weight of the legs. Table 2 shows the physical parameters of

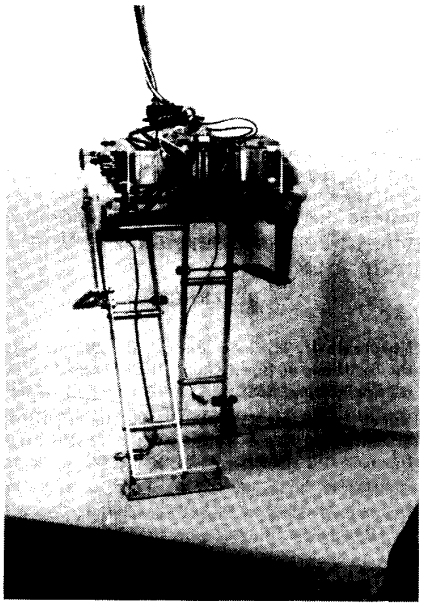

Fig. 10 Biped walking robot

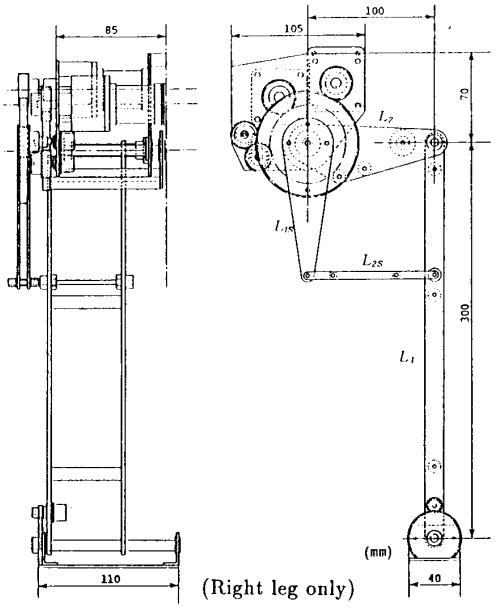

Fig. 11 Structure of the biped robot

Link	Mass(g)	Moment of Inertia (g.cm^2)
L_1	170	1.7×10^4
L_2	140	2.3×10^3
L_1s	100	9.3×10^2
L_2s	20	negligible
Body	1720	1.7×10^4
Foot	40	negligible

Table 2 Parameters of the experimental robot

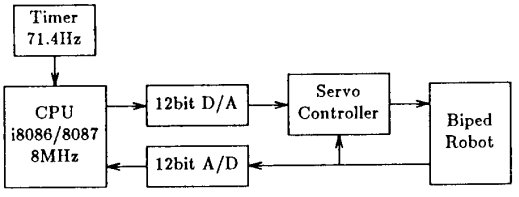

Fig. 12 Block diagram of the control system

the robot. The requirement that leg masses are nearly equal to zero is achieved to the following order:

(Transfer Leg Mass)/(Whole Mass) = 0.177

The overall block diagram of the control system is shown in Fig. 12. The servo controller controlls each joint of the legs based on the PD feedback (given by eq. (17)). Clock signals at 14 msec per cycle are input via I/O ports for the control program timing.

6.2 Adaptive Leg Exchange

To realize robust walking control, we have slightly changed the walking control algorithm. During the robot walking, the orbital energy can be calculated at every moment from the displacement x_g and the velocity $\dot{x}_g$ of the body.

$$E' = \frac{1}{2}\dot{x}_g^2 - \frac{g}{2y_h}x_g^2$$

If the robot had massless legs and there were no disturbances, E' would always be the specified constant value E_n. But in the case of the real robot, E' changes from E_n, affected by the motion of the transfer leg and many kinds of the disturbances. Therefore, the next leg exchange condition should be calculated from this E' (current orbital energy) and E_{n+1} (next desired orbital energy).

$$x_f' = \frac{y_h}{gs_{n+1}}(E_{n+1}-E') + \frac{s_{n+1}}{2} \qquad (20)$$

It is expected that after this adaptive leg exchange the specified trajectory of the next step can be realized even though the perturbation exists.

6.3 Software

Walking patterns are specified by step length, average speed, number of steps, starting condition, and stopping condition. The specific orbital energy E_n for each step is calculated from these parameters.

The walking control process executed every cycle (14 msec) contains (i) calculation and output of reference angles to maintain the specified height of the body and the vertical posture, (ii) the calculation of the position of the C.G. of the body x_g and the leg exchange condition x_f', and (iii) the control of the motion of the transfer leg. The support leg is exchanged when $x_g \geq x_f'$, and the transfer leg is controlled to touch the ground just at the exchange.

7. EXPERIMENTAL RESULTS

Two sets of data of the experiments are shown in Figs. 13 and 14. In both cases, five walking steps were specified from the walking start to a standstill. The height of the C.G. of the body was controlled at 36.0 cm from the ground, and the step width was specified to be 12.0 cm. An average target speed of 20 cm/sec was specified for experiment A and 30 cm/sec for experiment B. Figure 15 shows the walking motion in experiment B using a stick diagram representing only the support leg. In both experiments the biped failed to come to a standstill stop at the fifth support leg exchange and fell down. One of the causes was the occurrence of gradually excited rotative oscillation around the axis of walking direction that eventually grew to a level so severe that further steps become impossible. This oscillation was caused by the twisting of the legs, and it was difficult to prevent with our machine.

In Figs. 13 and 14, the velocity of the body stays unchanged at some of the leg exchanges as we assumed in Chapters 4 and 5. But at other exchanges, the velocity of the body decreases. The decrease is due to the uncontrollable impacts at the support leg exchange and we believe it can be eliminated with the use of more precise motion control or force control over the leg exchange.

The velocity of the body changes in a far more complex way than in the simulation and the orbital energy also deviates from the specified constant value (broken lines). We consider these facts are due to the motion of the transfer leg and the slight deviations in the height of the C.G. of the body (maximum 1.5 cm from the specified height).

Though such deviations from the ideal model existed, continuous walking motion was successfully achieved by means of the adaptive support leg exchange.

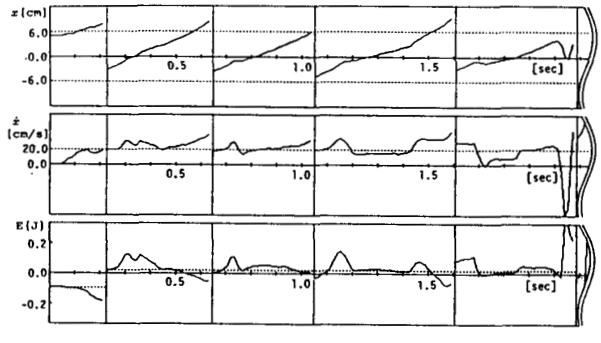

Fig. 13 Horizontal motion of the body (Experiment A)

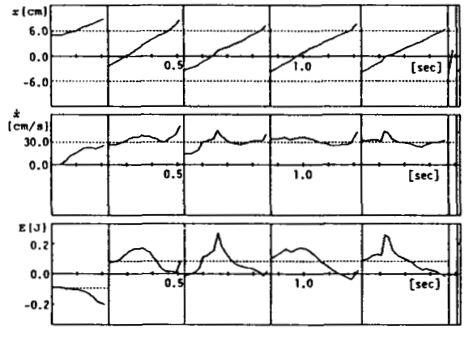

Fig. 14 Horizontal motion of the body (Experiment B)

8. CONCLUSIONS

To control dynamic walking of a biped robot, we proposed a potential energy conserving orbit, a special class of the trajectories of an ideal biped model. It has simple linear dynamics and is easy to analyze. Using the orbital energy derived from that linear dynamics, the walking motion can be designed easily. To make the walking motion robust, the attitude control using local feedback and the adaptive support leg exchange were proposed. We conducted experiments with a walking robot that was designed to approximate an ideal biped model. In our experiments, walk initiation and four continuous walking steps were achieved.

REFERNCES

[1] Vukobratović, M., and Juričić, D., "Contribution to the Synthesis of Biped Gait," IEEE Trans. on Biomedical Engineering, BME-16-1, 1969, pp.1-6

[2] Vukobratović, M., Frank, A.A, and Juričić, D., "On the Stability of Biped Locomotion," IEEE Trans. on Biomedical Engineering, BME-17-1, 1970, pp.25-36

[3] Gubina, F., Hemami, H., and McGhee, R.B., "On the Dynamic Stability of Biped Locomotion," IEEE Trans. on Biomedical Engineering, BME-21-2, 1974, pp.102-108.

[4] Golliday, C.L., and Hemami, H., "An Approach to Analyzing Biped Locomotion Dynamics and Designing Robot Locomotion Controls," IEEE Trans. on Automatic Control, AC-22-6, 1977, pp.963-972

[5] Miyazaki, F., and Arimoto, S., "A Control Theoretic Study on Dynamical Biped Locomotion," ASME Journal of Dynamic Systems, Measurement, and Control, Vol.102, 1980, pp.223-239

[6] Furusho, J., and Masubuchi, M., "A Theoretically Motivated Reduced Order Model for the Control of Dynamic Biped Locomotion," ASME Journal of Dynamic Systems, Measurement, and Control, Vol.109, 1987, pp.155-163

[7] Miura, H., Shimoyama, I., "Dynamic Walk of a Biped," The International Journal of Robotics Research, Vol.3, No.2, Summer 1984, pp.60-74

[8] Takanishi, A., Ishida, M., Yamazaki, Y., and Kato, I., "The Realization of Dynamic Walking by the Biped Walking Robot WL-10RD," Proceedings of '85 International Conference on Advanced Robotics (ICAR), 1985, pp.459-466

[9] Raibert, M.H., "Legged robots that balance," Cambridge: MIT Press, 1986

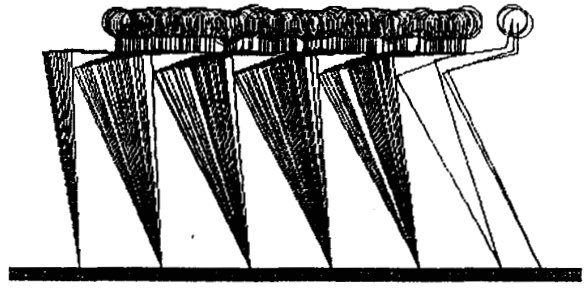

Fig. 15 Stick diagram (Experiment B)